

Geometrically induced modification of surface plasmons in the optical and telecom regimes

M. L. Nesterov,^{1,2,*} D. Martin-Cano,¹ A. I. Fernandez-Dominguez,^{1,†}

E. Moreno,¹ L. Martin-Moreno,³ and F. J. Garcia-Vidal^{1,‡}

¹*Departamento de Física Teórica de la Materia Condensada,
Universidad Autónoma de Madrid,
E-28049 Madrid, Spain*

²*A. Ya. Usikov Institute for Radiophysics and Electronics NAS of Ukraine,
12 Academician Proskura Street, 61085 Kharkov, Ukraine*

³*Instituto de Ciencia de Materiales de Aragón (ICMA) and Departamento de Física de la Materia Condensada,
CSIC-Universidad de Zaragoza, E-50009 Zaragoza, Spain*

*Corresponding author: nesterovml@gmail.com

‡Electronic address: fj.garcia@uam.es

(Dated: October 25, 2021)

We demonstrate that the introduction of a subwavelength periodic modulation into a metallic structure strongly modifies the guiding characteristics of the surface plasmon modes supported by the system. Moreover, it is also shown how a new type of a tightly confined surface plasmon polariton mode can be created by just milling a periodic corrugation into a metallic ridge placed on top of a metal surface.

Photonics based on the exciting capabilities of surface plasmon polaritons (SPPs) has become a very active area of research during the last decade [1–3]. Strong localization of electromagnetic (EM) fields and the building up of ultra-small SPP-based waveguides [4, 5] have been achieved thanks to the subwavelength (the term “sub-wavelength” refers to the vacuum wavelength) nature of the SPP fields, thus enabling a great variety of applications in optics [6, 7].

However, in order to fulfill the potentialities of light guiding based on SPP excitation, it is convenient to search for effective ways to control and tune the propagation characteristics of SPP modes. The concept of geometrically-induced SPPs [8–13] (also named *spoof* SPPs) has proven to be very powerful in tailoring the dispersion relation of the propagating surface EM modes in the microwave and terahertz regimes. The aim of this Letter is to transfer the spoof SPP concept to the optical and telecom ranges. We will demonstrate how the dispersion relation of propagating SPP modes can be tuned by introducing a periodic modulation in the metal surface in a length scale much smaller than the wavelength (λ). Even more, we will show how this modulation could also “build-up” tightly confined SPP modes in structures where these modes were not supported in the non-corrugated case.

First we consider a SPP mode that is bound to and propagates along a finite V-shaped groove milled in a metal film, the so-called channel plasmon polariton (CPP). The propagation characteristics of these CPP modes have been studied both theoretically [14–16] and experimentally [17] during the last years, and even prototype CPP-based photonic circuits have been already fabricated [18]. In Fig. 1(a) we plot the dispersion relation (frequency versus parallel momentum) of the fun-

damental CPP mode for a V-groove whose geometrical parameters are taken from experiments [19]. The metal considered is gold and its frequency-dependent dielectric function is taken from [20]. All the numerical calculations presented in this paper have been performed using a Finite Element Method (FEM). Due to the finite depth of the grooves, this CPP mode presents a cutoff wavelength that, for the chosen set of geometrical parameters (see caption of Fig. 1), appears at around $1.3\ \mu\text{m}$. Grey curves in Fig. 1(a) illustrate the modification of the CPP dispersion relation induced by a sub- λ periodic modulation in the V-groove. The main effect of the corrugation is to shift the cutoff wavelength of the CPP mode to longer wavelengths, reaching a value of $1.6\ \mu\text{m}$ for the shortest period analyzed, $d = 25\ \text{nm}$. Also, as its dispersion relation departs more from the light line, the CPP for the corrugated V-groove becomes more localized than the *pure* one.

Our finding that cutoff wavelength shifts to longer wavelengths in corrugated V-grooves could explain why in the experiments there exists a propagating CPP mode in the wavelength range between 1424–1640 nm [17], despite the fact that calculations for a non-corrugated V-groove with the same geometrical parameters ($\theta = 25$ degrees) predict a cutoff wavelength of 1440 nm [16]. Scanning electron microscope images reveal the presence of a weak periodic modulation in V-grooves fabricated with focused ion beam techniques. When a shallow corrugation with a period $d = 25\ \text{nm}$ is now introduced in the V-groove, our calculations show that the cutoff wavelength moves from 1440 nm to 1750 nm, larger than the wavelength range analyzed in the experiments.

A much stronger effect associated with a longitudinal sub- λ periodic corrugation is seen for another type of SPP modes: a slot SPP mode that propagates along a

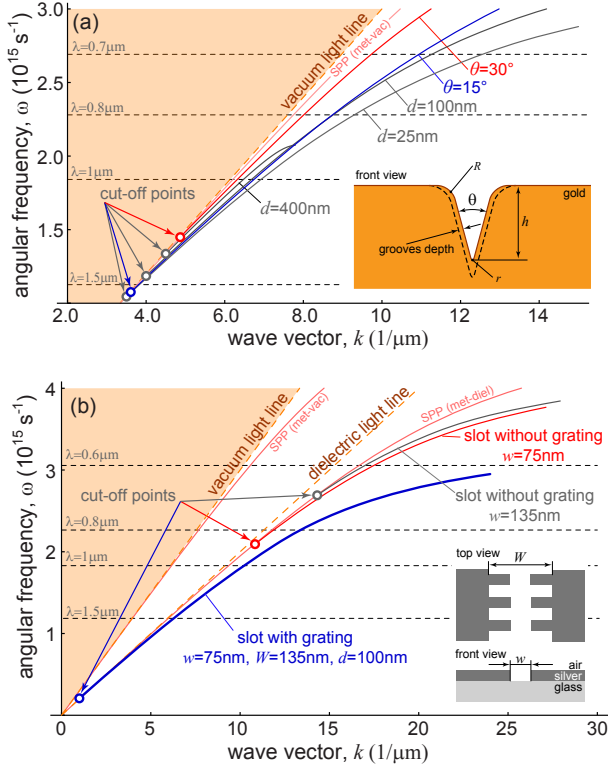


FIG. 1. (a) Dispersion curves for CPPs. Red and blue curves represent those for a CPP mode of the V-groove without corrugation for two different angles, $\theta = 30^\circ$ and $\theta = 15^\circ$. The depth of the V-groove is $h = 1.1 \mu\text{m}$ and the radii of curvature at the edges are $r = 10 \text{ nm}$ and $R = 100 \text{ nm}$. Grey lines display the dispersion curves for CPP modes of the corrugated V-groove ($\theta = 30^\circ$) where the depth of the grating is fixed at 30 nm and three different periods are studied: $d = 400 \text{ nm}$, $d = 100 \text{ nm}$ and $d = 25 \text{ nm}$. Inset shows the geometry. (b) Dispersion curves for slot waveguide modes. Red and grey curves are those for the slot without grating. Blue curve is the dispersion curve for a corrugated slot. The period of the grating is $d = 100 \text{ nm}$.

gap carved between two metal plates. Here we consider a waveguide structure that is composed of a slot perforated on a thin silver film deposited on top of a glass substrate ($\epsilon = 2.25$), see inset of Fig. 1(b). The main geometrical parameter that controls the dispersion relation of these modes is the width of the slot, w . Figure 1(b) shows two different non-corrugated structures, $w_1 = 75 \text{ nm}$ (red line) and $w_2 = 135 \text{ nm}$ (grey line). The geometry of the corrugation is chosen so the distance between two deepest points, W , is equal to w_2 whereas the minimal distance is equal to w_1 , see inset of Fig. 1(b). The introduction of a periodic modulation has a dramatic effect on the dispersion relation. One could naively expect that the resulting dispersion curve would be located between those for the non-corrugated cases. However, the band for the corrugated slot departs strongly from those two curves,

resulting in a much longer cutoff wavelength and larger confinement. Then, our results clearly show that a sub- λ periodic modulation could also be used to improve the guiding properties of slot waveguide modes.

Now we demonstrate that a sub- λ periodic modulation could indeed create a SPP mode in structures where, without corrugation, laterally confined SPP modes are not supported. As an example we consider a metallic ridge (height h and width L) placed on top of a substrate made of the same metal, see Fig. 2(b). This structure does not support the propagation of SPP modes transversally localized. In Fig. 2(a) we render the dispersion relations of the geometrically-induced SPP modes that emerge when a sub- λ periodic modulation is introduced into a gold ridge. The six curves correspond to different values of the modulation depth, g . As clearly seen in the figure, even the weakest modulation ($g = 20 \text{ nm}$) is able to create a laterally confined SPP mode (i.e., the dispersion curve is lower than the SPP-curve for the flat metal surface). When the depth is enlarged, the dispersion relation further departs from the light line, increasing the mode localization. Accompanying this movement, the cutoff frequency shifts to lower frequencies. The increase in the mode localization also affects the propagation length of these geometrically-induced SPP modes. For a fixed wavelength, the transversally confined mode decays faster for a larger g , see Fig. 2(c).

In the case where the grating depth is equal to the height of the slab, the geometry resembles a 1D chain of metallic box-shaped particles placed on top of a metal film. From now on, we name the mode supported by this structure as *Domino Plasmon-Polariton* (DPP). This DPP mode has a high electric field localization near the top part of the domino structure, see Fig. 3. In this figure the horizontal slice renders the electric field intensity evaluated in a xz -plane that is parallel to the metal substrate and located 5 nm above the domino's top face. The intensity also presents a strong subwavelength confinement in the transversal direction. Regarding the vectorial nature of the EM-fields associated with a DPP, the electric field has mainly y and z components (see yellow lines in the vertical plane of Fig. 3) whereas the magnetic field has predominant x and z components (see blue lines in the horizontal plane of Fig. 3).

It is worth discussing the differences between the DPP modes described above and the plasmon modes supported by 1D arrays of metal nanoparticles placed on top of a dielectric film [21, 22]. In this last case, the near-field coupling between the localized plasmon modes of the metal nanoparticles leads to the formation of a very flat plasmon band characterized by a deep sub- λ confinement but short propagation length. However, in the case of DPP modes, the presence of the metal substrate results in the emergence of a "polaritonic" part in the dispersion relation that runs close to the SPP band of the flat surface [see Fig. 2(a)]. Accordingly, DPP modes

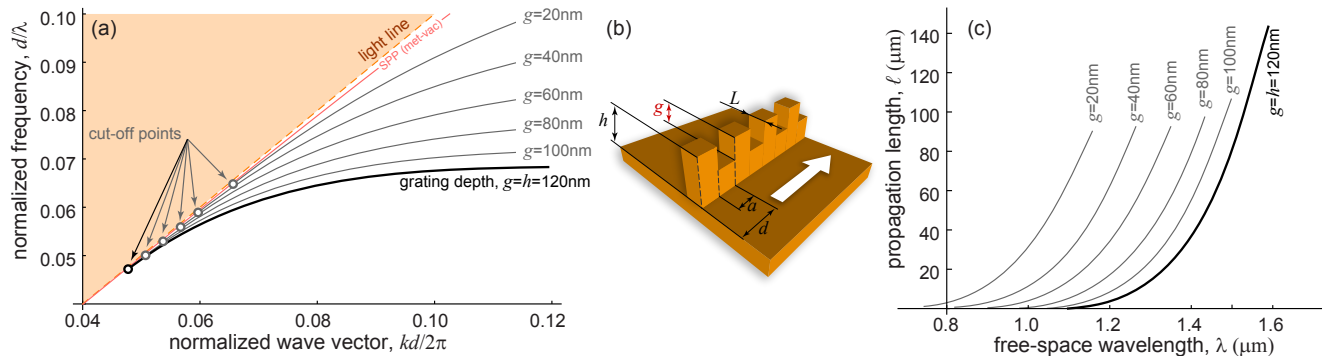


FIG. 2. Creation of a geometrically-induced ridge SPP mode. (a) Dispersion curves for SPP modes running on a corrugated ridge with different modulation depths. (b) Geometry of the ridge structure with a modulation: corrugation period $d = 75$ nm, width of the ridge $L = 37.5$ nm, height of the ridge $h = 120$ nm and the grooves width $a = d/2 = 37.5$ nm. (c) Corresponding propagation lengths for the cases analyzed in panel (a).

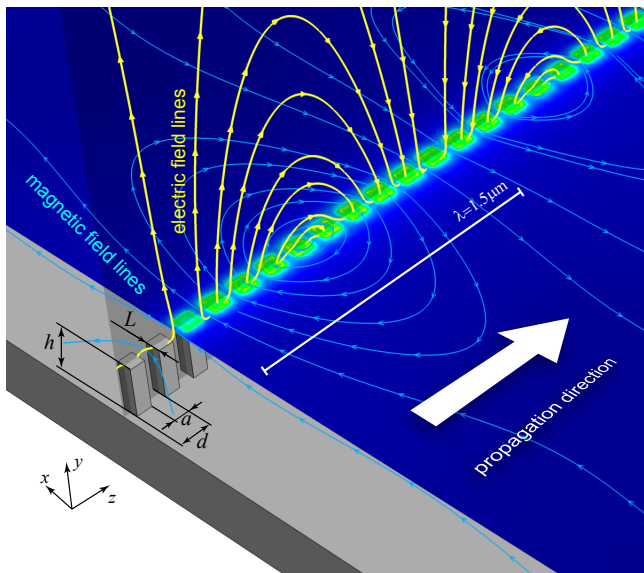


FIG. 3. Electric and magnetic fields associated with a domino plasmon polariton mode. Yellow (blue) lines represent the electric (magnetic) vector field. Electric field intensity map is evaluated on a horizontal plane located on top of the domino structure. The geometrical parameters of the domino structure are: modulation period $d = 75$ nm, lateral width of the ridge $L = 37.5$ nm, height $h = 120$ nm and the grooves' width $a = d/2$. The operating wavelength is $\lambda = 1.5 \mu\text{m}$. The definition of the cartesian axes is also depicted.

operating within this polaritonic regime poses a very long propagation length but, as expected, are much less confined than the modes supported by a chain of metal nanoparticles.

The propagation properties of a DPP mode depend on the lateral size (L) of the structure. By varying this dimension we could find optimal properties of the DPP mode, like enhanced field confinement and/or longer propagation length. Figure 4(a) shows the DPP disper-

sion curves for four different values of L . As this width is reduced from $L = \infty$ to $L = 0.5d = 37.5$ nm, the cutoff frequency increases and, for a fixed frequency, the wavevector is smaller for narrower dominos. Accordingly, the DPP propagation length for very narrow dominos is larger than that for a wider one (see Fig. 4(b)). Interestingly, even for a domino width of only $L = d/2 = 37.5$ nm the propagation length at $\lambda = 1.5 \mu\text{m}$ is around $80 \mu\text{m}$, a value that is larger than those predicted for other types of SPP modes that present sub- λ confinement like CPPs [16] or wedge plasmon polaritons [23]. When the metal behaves as a perfect electrical conductor, our calculations show that the dispersion relation of the DPP mode is almost independent of L , paving the way to several interesting applications for the use of DPPs in the terahertz regime [24].

Figures 4(c-e) render the electric field intensity distribution for three DPPs in a plane perpendicular to the propagation direction located at the center of the gap between two dominos. The lateral sizes analyzed are $L = 0.5d$, $L = 3.5d$ and $L = 10d$ and the operating wavelength is $\lambda = 1.5 \mu\text{m}$. The color scale is the same for the three distributions. As expected from the dispersion curves, the DPP mode is more confined for the wider domino, $L = 10d$. When the domino width is decreased, the EM energy is carried within a bigger volume. This is illustrated in Figs. 4(c-e) by representing the energy isocurves for the three different dominos. The percentage associated with each isocurve measures the amount of EM energy (with respect to the total one) carried out through the area inscribed into the curve. This is the usual way to define the modal size of a waveguide mode [25]. However, a closer look at the intensity distributions shows that the electric field in the case $L = 3.5d$ presents a stronger field localization than the $L = 10d$ or $L = 0.5d$ cases. Nevertheless, a comparison of electric field distributions with the operating wavelength (white

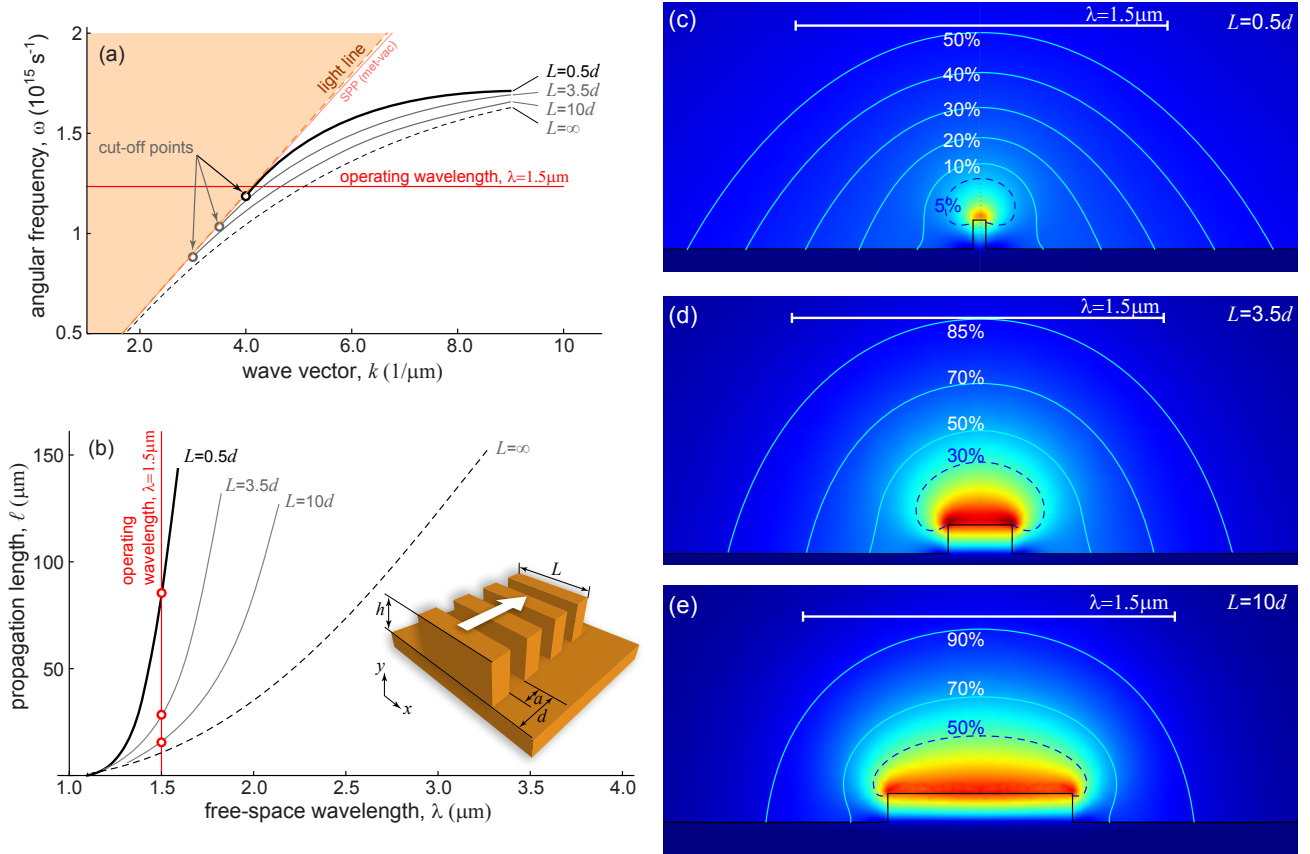


FIG. 4. Dependence of the DPP propagation characteristics with the domino width. (a) Dispersion curves of the DPP modes for four different widths L of the structure. The geometrical parameters of the domino structure are the same as in previous figures. (b) Propagation length versus free-space wavelength for the four structures analyzed in panel (a). (c-e) Electric field intensity distributions evaluated at $\lambda = 1.5 \mu\text{m}$ in a plane perpendicular to the propagation direction for three different values of L . The blue lines show several energy isocurves: the percentage measures the amount of energy (with respect to total one) carried through the area bounded by the corresponding isocurve.

bars) in Fig. 4 illustrates the strong sub- λ transversal confinement associated with the propagation of DPP modes.

In conclusion, we have shown that the application of the spoof plasmon concept in the optical and telecom regimes allows tailoring of the guiding properties of SPP modes. Moreover, we have also demonstrated that the same approach leads to the emergence of guided modes in geometries where conventional SPPs are not supported. We have illustrated this finding by analyzing the so-called Domino Plasmon Polaritons, which exhibit an excellent trade-off between lateral confinement and propagation length.

This work was sponsored by the the Spanish Ministry of Science under projects MAT2009-06609-C02 and No. CSD2007-046-NanoLight.es.

- [1] W. L. Barnes, A. Dereux, and T. W. Ebbesen, *Nature* **424**, 824 (2003).
- [2] A. V. Zayats, I. I. Smolyaninov, and A. A. Maradudin, *Phys. Rep.* **408**, 131 (2005).
- [3] S. A. Maier, *Plasmonics: fundamentals and applications* (Springer, 2007).
- [4] R. Buckley and P. Berini, *Opt. Express* **15**, 12174 (2007).
- [5] S. I. Bozhevolnyi, *Plasmonic nanoguides and circuits* (World Scientific, 2009).
- [6] H. Ditlbacher, J. R. Krenn, G. Schider, A. Leitner, and F. R. Aussenegg, *Appl. Phys. Lett.* **81**, 1762 (2002).
- [7] T. W. Ebbesen, C. Genet, and S. I. Bozhevolnyi, *Phys. Today* **61**(5), 44 (2008).
- [8] J. B. Pendry, L. Martin-Moreno, and F. J. Garcia-Vidal, *Science* **305**, 847 (2004).
- [9] A. P. Hibbins, B. R. Evans, and J. R. Sambles, *Science* **308**, 670 (2005).
- [10] F. J. Garcia de Abajo and J. J. Saenz, *Phys. Rev. Lett.* **95**, 233901 (2005).
- [11] S. A. Maier, S. R. Andrews, L. Martin-Moreno, and F. J. Garcia-Vidal, *Phys. Rev. Lett.* **97**, 176805 (2006).

- [12] C. R. Williams, S. R. Andrews, S. A. Maier, A. I. Fernández-Domínguez, L. Martín-Moreno, and F. J. García-Vidal, *Nat. Photonics* **2**, 175 (2008).
- [13] A.I. Fernández-Domínguez, E. Moreno, L. Martín-Moreno, and F.J. García-Vidal, *Opt. Lett.* **34**, 2063 (2009).
- [14] I. V. Novikov and A. A. Maradudin, *Phys. Rev. B* **66**, 035403 (2002).
- [15] D. F. P. Pile and D. K. Gramotnev, *Opt. Lett.* **29**, 1069 (2004).
- [16] E. Moreno, F. J. García-Vidal, S. G. Rodrigo, L. Martín-Moreno, and S. I. Bozhevolnyi, *Opt. Lett.* **31**, 3447 (2006).
- [17] S. I. Bozhevolnyi, V. S. Volkov, E. Devaux, and T. W. Ebbesen, *Phys. Rev. Lett.* **95**, 046802 (2005).
- [18] S. I. Bozhevolnyi, V. S. Volkov, E. Devaux, J. Y. Laluet, and T. W. Ebbesen, *Nature* **440**, 508 (2006).
- [19] S. I. Bozhevolnyi, V. S. Volkov, E. Devaux, J.-Y. Laluet, and T. W. Ebbesen, *Appl. Phys. A* **89**, 225 (2007).
- [20] A. Vial, A. S. Grimault, D. Macias, D. Barchiesi, and M. L. de la Chapelle, *Phys. Rev. B* **71**, 085416 (2005).
- [21] J. R. Krenn, A. Dereux, J. C. Weeber, E. Bourillot, Y. Lacroute, J. P. Goudonnet, G. Schider, W. Gotschy, A. Leitner, and F. R. Aussenegg, *Phys. Rev. Lett.* **82**, 2590 (1999).
- [22] S. A. Maier, P. G. Kik, H. A. Atwater, S. Meltzer, E. Harel, B. E. Koel, and A. A. G. Requicha, *Nature Mat.* **2**, 229 (2003).
- [23] E. Moreno, S. G. Rodrigo, S. I. Bozhevolnyi, L. Martín-Moreno, and F. J. Garca-Vidal, *Phys. Rev. Lett.* **100**, 023901 (2008).
- [24] D. Martín-Cano, M. L. Nesterov, A. I. Fernández-Domínguez, F. J. García-Vidal, L. Martín-Moreno, and E. Moreno, *Optics Express* **18**, 754 (2010).
- [25] R. F. Oulton, G. Bartal, D. F. P. Pile, and X. Zhang, *New J. Phys.* **10**, 105018 (2008).